UDC 621.3.013 https://doi.org/10.20998/2074-272X.2024.6.04

C.D. Tran, M. Kuchar, P.D. Nguyen

Research for an enhanced fault-tolerant solution against the current sensor fault types in induction motor drives

Introduction. *Recently, three-phase induction motor drives have been widely used in industrial applications; however, the feedback signal failures of current sensors can seriously degrade the operation performance of the entire drive system. Therefore, the motor drives require a proper solution to prevent current sensor faults and improve the reliability of the motor drive systems.* ***The novelty*** *of the proposed research includes integrating the current sensor fault-tolerant control (FTC) function according to enhanced technique into the field-oriented control loop for speed control of the motor drive system.* ***Purpose.*** *This research proposes a hybrid method involving a third difference operator and signal comparison algorithm to diagnose various types of current sensor faults as a positive solution to enhance the stability of the induction motor drive system.* ***Methods.*** *A hybrid method involving a third difference operator for the measured speed signals and a comparison algorithm between measured and estimated current signals are proposed to diagnose the current sensors' health status in the fault-tolerant process. After determining the faulty sensor, the estimated current signals based on the Luenberger observer are used immediately to replace the defective sensor signal.* ***Results.*** *The current sensor is simulated with various failure types, from standard to rare failures, to evaluate the performance of the FTC method implemented in the MATLAB/Simulink environment. Simultaneously, a fault flag corresponding to a defective sensor should be presented as an indicator to execute the repair process for faulty sensors at the proper time.* ***Practical value.*** *Positive results have proven the feasibility and effectiveness of the proposed FTC integrated into the speed controller to improve reliability and ensure the stable operation of the induction motor drive system even under current sensor fault conditions.* References 29, tables 3, figures 10.

Key words: **current sensor fault, estimated current, fault-tolerant control, field-oriented control, induction motor drive.**

Вступ. *Останнім часом трифазні приводи з асинхронними двигунами широко використовуються у промисловості; однак відмови сигналу зворотного зв'язку датчиків струму можуть погіршити експлуатаційні характеристики всієї системи приводу. Тому для електроприводів потрібне належне рішення для запобігання відмов датчиків струму та підвищення надійності систем приводу.* ***Новизна*** *пропонованого дослідження полягає в інтеграції функції відмовостійкого управління датчиком струму (FTC) відповідно до вдосконаленої методики в контур управління полем для управління швидкістю системи приводу.* ***Мета***. *У цьому дослідженні пропонується гібридний метод, що включає оператор третьої різниці та алгоритм порівняння сигналів для діагностики різних типів відмов датчиків струму як позитивне рішення для підвищення стійкості системи приводу з асинхронним двигуном.* ***Методи***. *Пропонується гібридний метод, що включає оператор третьої різниці для виміряних сигналів швидкості та алгоритм порівняння між виміряними та оціночними сигналами струму, для діагностики стану справності датчиків струму у відмовостійкому процесі. Після визначення несправного датчика сигнали оцінки струму на основі спостерігача Люенбергера негайно використовуються для заміни сигналу несправного датчика.* ***Результати***. *Датчик струму моделюється з різними типами відмов, від стандартних до рідкісних відмов, з метою оцінки продуктивності методу FTC, реалізованого у середовищі MATLAB/Simulink. Одночасно прапорець несправності, що відповідає несправному датчику, повинен бути представлений як індикатор для виконання процесу ремонту несправних датчиків у належний час.* ***Практична цінність***. *Позитивні результати довели здійсненність та ефективність пропонованого FTC, інтегрованого в регулятор швидкості, для підвищення надійності та забезпечення стабільної роботи системи приводу з асинхронним двигуном навіть в умовах несправності датчика струму..* Бібл. 29, табл. 3, рис. 10.

Ключові слова: **несправність датчика струму, розрахунковий струм, відмовостійке керування, орієнтоване на поле керування, привід з асинхронним двигуном.**

Introduction. Three-phase induction motors (3~IM) with the advantages of size, reliability, performance, and flexible control are currently widely used electrical machines in various fields [1, 2], such as industry, transportation, agriculture and so on. A system that includes a 3~IM connecting to the load, an inverter power, a sensor system, and a controller is called the induction motor drive (IMD). Modern speed control techniques applying inverter technology for IMD include two primary control groups: scalar and vector technique control [3, 4]. The principle of the scalar control method is based on keeping the flux according to the *V/f* ratio. This method has advantages: it is a simple control algorithm and has a low cost. However, the control performance is low and only used for simple applications. In contrast, the group of vector control methods, typically the field-oriented control (FOC) method, has high performance, but complex control algorithms and high costs are used for applications requiring high precision [5, 6]. Modern 3~IMD structure includes four main parts: motor, voltage source inverter, controller integrated control algorithm, and sensor system.

Problems and the relevance. All of the parts in the IMD's structure play an essential role in the system's stable operation. Hence, the accuracy of the sensors is vital to ensuring the stability of the drive system [7, 8]. Loss of connection or accuracy of sensor feedback signals can lead to function degradation or damage to the motor drive system. Therefore, it is necessary to develop functions against sensor faults to improve the reliability of the motor drive system; the function is called the fault-tolerant control (FTC) technique [9, 10]. A comprehensive sensor FTC function includes three distinct processes: fault diagnosis, fault signal isolation, and reconfiguration to maintain stable operation under fault conditions. During the fault diagnosis stage, the health status of the sensor should be determined, and any faulty sensor needs to be accurately located. Faulty sensors must be isolated immediately whenever a fault condition is identified. Immediately, the signal from this faulty sensor must be replaced with an estimated signal; in other words, switch from sensor control mode to sensorless control [11, 12].

Review of recent publications about the FTC and unsolved tasks. The sensor system in the motor drive system includes two types of sensors: the current sensor and the speed sensor. Therefore, research on sensor faults is also divided into two subjects: the speed sensor fault (SSF)

and the current sensor fault (CSF). Most research on sensor FTC focuses on completely damaged or disconnected faults, where the feedback signals to the controller become zero. Corresponding to this fault type, with SSF cases, diagnosis methods mainly rely on comparison algorithms between measured and estimated signals [13–15]; with the CSF cases, various techniques exist for diagnosing sensor failures, such as relying on the difference between the measured signal and the estimated signal [16], phase imbalance and missing error phase [17], or sudden changes in the measured signal [18, 19], or using a mixed evaluation index [20]. However, besides total damaged failure, several other types of fault can occur for current sensors, but most studies pay little attention to them.

Purpose of the paper. This research proposes a hybrid method involving a third difference operator (TDO) and signal comparison algorithm [21] to diagnose various types of current sensor faults, such as bias, drift, and gain fault [22] as a positive solution to enhance the stability of the IMD system. Once the faulty sensor is identified, current signals estimated based on direct estimators [23, 24] or observers like Luenberger [25, 26] are used instead of the faulty current signal.

FTC solution against the current sensor failure for 3~IMDs. This section briefly describes an IMD model integrating the current sensor-FTC function, various types of CSF, and the applied FTC algorithm. The motor modeling operations and the Clarke and Park transformations are also summarized to clarify the proposed FTC solution.

A. IMD model integrating the current sensor FTC function. The structure of the IMD includes a 3~IM connecting to the load, an inverter power, a sensor system, and a controller (Fig. 1). An FTC algorithm is integrated into the controller function to enhance the CSF protection feature (Fig. 1). FTC block receives the stator current and rotor speed as input signals for calculating the corresponding estimated quantities to implement the fault diagnosis algorithm (Fig. 2).

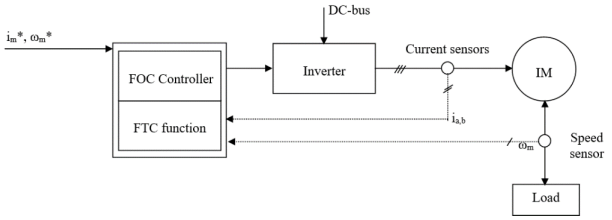

Fig. 1. 3~IMD integrated FTC function

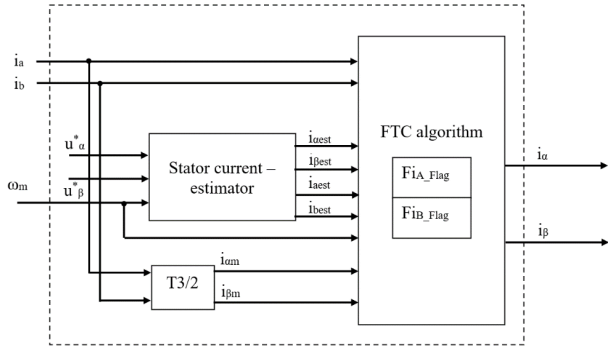

Fig. 2. FTC function block

In the FTC function block, the current estimator receives the measured motor speed and calculated stator voltage from the DC-link, combining inverter switching impulse [27] to generate the estimated current by proper methods. The estimated and measured current signals are provided for implementing the CSF diagnosis algorithm [21] and providing proper current signals to the FOC controller. The estimation equation system of the virtual currents based on the Luenberger observer [28, 29] is presented briefly below:

$$\frac{di_{S\alpha}}{dt} = -E_1 i_{S\alpha} + E_2 \psi_{R\alpha} + E_3 \psi_{R\beta} + E_4 u^*_{S\alpha} - L_1 i_{S\alpha} + L_2 i_{S\beta}; \quad (1)$$

$$\frac{di_{S\beta}}{dt} = -E_1 i_{S\beta} - E_3 \psi_{R\alpha} + E_2 \psi_{R\beta} + E_4 u^*_{S\beta} - L_1 i_{S\beta} - L_2 i_{S\alpha}; \quad (2)$$

$$\frac{d\psi_{R\alpha}}{dt} = E_5 i_{S\alpha} - E_6 \psi_{R\alpha} - E_7 \psi_{R\beta} - L_3 i_{S\alpha} + L_4 i_{S\beta}; \quad (3)$$

$$\frac{d\psi_{R\beta}}{dt} = E_5 i_{S\beta} + E_7 \psi_{R\alpha} - E_6 \psi_{R\beta} + L_3 i_{S\beta} - L_4 i_{S\alpha}; \quad (4)$$

where

$$E_1 = \frac{\left(L_R^2 R_S + L_m^2 R_R\right)}{\sigma L_S L_R^2}; \quad E_2 = \frac{L_m R_R}{\sigma L_S L_R^2}; \quad E_3 = \frac{L_m \omega_r}{\sigma L_S L_R};$$

$$E_4 = \frac{1}{\sigma L_S}; \quad E_5 = \frac{L_m R_R}{L_R}; \quad E_6 = \frac{R_R}{L_R}; \quad E_7 = \omega_r;$$

$$L_1 = (h-1)\left(\frac{1}{\sigma T_S} + \frac{1}{\sigma T_R}\right); \quad L_2 = -(h-1)\omega_r;$$

$$L_3 = \left(h^2 - 1\right)\left[\left(\frac{1}{\sigma T_S} + \frac{1}{\sigma T_R}\right)\frac{\sigma L_m L_S}{L_R} - \frac{L_m}{T_R}\right] +$$

$$+ \frac{\sigma L_m L_S}{L_R}\left(\frac{1}{\sigma T_S} + \frac{1}{\sigma T_R}\right)(h-1);$$

$$L_4 = -(h-1)\frac{\sigma L_m L_S}{L_R}\omega_r; \quad T_S = \frac{L_S}{R_S}; \quad T_R = \frac{L_R}{R_R};$$

$$\sigma = \frac{L_S L_R - L_m^2}{L_S L_R}; \quad h = \text{const} > 1;$$

R_S, R_R are the stator and rotor resistance; L_S, L_R, L_m are the stator, rotor and magnetizing inductance; $\omega_r = p\omega_m$ is the rotor speed; p is the number of pole pairs; $i_{S\alpha}$, $i_{S\beta}$, $u^*_{S\alpha}$, $u^*_{S\beta}$, $\psi_{R\alpha}$, $\psi_{R\beta}$, are the stator current, voltage and rotor flux components in the stationary frame;

The real-time stator current can be converted to the stationary coordinate system using the Clarke formula (5) and the inverse transformation (6):

$$\begin{bmatrix} i_\alpha \\ i_\beta \end{bmatrix} = \begin{bmatrix} 1 & 0 \\ 1/\sqrt{3} & 2/\sqrt{3} \end{bmatrix} \begin{bmatrix} i_a \\ i_b \end{bmatrix}; \quad (5)$$

$$\begin{bmatrix} i_a \\ i_b \end{bmatrix} = \begin{bmatrix} 1 & 0 \\ -1/2 & \sqrt{3}/2 \end{bmatrix} \begin{bmatrix} i_\alpha \\ i_\beta \end{bmatrix}. \quad (6)$$

B. Current sensor failure types. During the operation of the IMD, under the influence of various factors of the operating environment such as temperature, vibration, electromagnetic field impact, and deterioration of equipment life, sensors may be damaged or degraded function. A sensor is considered faulty when its signal to the controller seriously deviates beyond the available threshold compared with the actual signal. Some typical types of sensor faults considered in the FTC technique correspond to soft fault type: drift, scale, bias, precision degradation, and

hard fault type (total failures): constant feedback value, constant feedback value with noise, and bottom noise [22]. Suppose the measurement standard deviation of the sensors is ignored. In that case, the mathematical expressions describing the sensor fault types are presented in Table 1 and Fig. 3 according to the types of CSF signals.

Table 1

Mathematical expressions according to sensor fault types

Type	Expression	Note
Soft fault		- $i_m(t)$ is the measured phase current corresponding to the fault type; - $i(t)$ is the true value of the measured phase current; - a, b, K are the constants corresponding to the fault type; - $e(t)$ is the excessive random noise; - t is the time variable
Drift	$i_m(t)=i(t)+a+bt$	
Scale	$i_m(t)=Ki(t)$	
Bias	$i_m(t)=i(t)+K$	
Precision degradation	$i_m(t)=i(t)+e(t)$	
Hard fault		
Constant	$i_m(t)=K$	
Constant with noise	$i_m(t)=K+e(t)$	
Bottom noise	$i_m(t)=0+e(t)$	

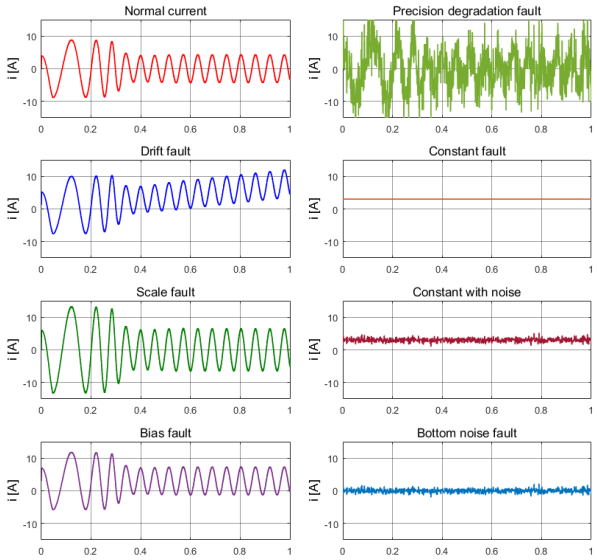

Fig. 3. Graphical signals of healthy state and fault state types of the phase current

C. FTC against current sensor failures. A hybrid method involving a TDO for the measured rotor speed and a comparison algorithm of estimated and measured current signals is applied to diagnose the current sensors' health status. First, the TDO algorithm corresponding to (7) is used to check whether there are signs of failure with the speed sensor:

$$\text{If } (TDO_w \geq Th_w)\ \{F_{TDO_w} = 1\}, \quad (7)$$

where $TDO_w = \left|\Delta^3 w(p)\right|$;

$$\begin{cases} 1^{\text{st}}\text{ operator}: \Delta^1 w(p) = w(p) - w(p-1); \\ 2^{\text{nd}}\text{ operator}: \Delta^2 w(p) = \Delta^1 w(p) - \Delta^1 w(p-1); \\ 3^{\text{rd}}\text{ operator}: \Delta^3 w(p) = \Delta^2 w(p) - \Delta^2 w(p-1); \end{cases}$$

where p is the current sampling time; $(p–1)$ is the previous sampling time; Th_w is the defined threshold selected to determine the fault state of the speed sensors. The threshold can be chosen with a value 10 % corresponding to the reference speed, as shown in [21].

Then, suppose the measured speed signal is determined the normality state. In that case, the estimated and measured signal comparison algorithms are implemented to check the current sensor faults, as in (8) and (9):

$$\text{If } \left(\left|i_{j-m} - i_{j-est}\right| > Th_i\right)\{F_{COMj} = 1\};\ \text{else } \{F_{COMj} = 0\}, \quad (8)$$

$$\text{If } \left(\left(!F_{TDO_w}\right)\text{and } F_{COMj}\right) = 1;\ \{F_j = 1\};\ \text{else } \{F_j = 0\}, \quad (9)$$

where $i_{j–m}$ are the measured current signals of i_a, i_b; $i_{j–est}$ is the estimated current signals of $i_{a\ est}$, $i_{b\ est}$; F_j is the fault indication flag for each current sensor; Th_i is the threshold selected to determine the fault state of the current sensor with a value 10 %.

Remark: The «NOT» operator in (9) ensures that the measured rotor speed signal is in good condition, which means the estimated current signal is correct.

If the fault indication flags are low, the FTC function will transfer the feedback-measured current to the FOC controller. Otherwise, if the fault indication flags are high, the FTC unit will provide the corresponding estimated current signals for the speed control in IMD. The principle of the FTC unit is shown in Table 2.

Table 2

Judgment of FTC function

Fault indication flag	Current sensor status	The output
$F_{IA} = 0, F_{IB} = 0$	Normal	$i_{\alpha m}, i_{\beta m}$
$F_{IA} = 1, F_{IB} = 0$	A-phase fault	$i_{\alpha\,est}, i_{\beta\,est}$
$F_{IA} = 0, F_{IB} = 1$	B-phase fault	$i_{\alpha\,est}, i_{\beta\,est}$

Simulation results. The operation of the 3~IMD using the FOC method is carried out in the normal speed zones, and the failures corresponding to seven types of current faults are simulated to evaluate the performance of the FTC solution integrated into the controller. The machine parameters of the motor are shown in Table 3.

Table 3

Parameters of the induction motor

Rated power, W	2200
Rated voltage, V	400
Nominal speed, rpm	1420
Pole pairs number	2
Stator resistance, Ω	3.179
Rotor resistance, Ω	2.118
Stator inductance, H	0.209
Rotor inductance, H	0.209
Magnetizing inductance, H	0.192

A reference speed will be set, including acceleration from 0 to 500 rpm in 0.3 s, and kept constant throughout the operation. CSF types are simulated to test the speed controller's FTC performance. Corresponding to the soft faults of the current sensors, drift fault, scale fault, bias fault, and precision degradation are simulated to investigate the performance of the proposed FTC method.

In Fig. 4, the motor is operating stably; when 1.2 s a drift-fault occurs at phase A (Fig. 4,*a*), the FTC function immediately operates to diagnose the fault accurately and quickly, and the phase A current fault flag is pushed high while the corresponding phase B fault flag remains low (Fig. 4,*b*). The estimated current replaces the measured current signal, making the IMD stable.

In Fig. 5, similar to the first case, a scale fault occurs at phase B (Fig. 5,*a*); the FTC function immediately operates to diagnose the scale fault at the fault phase, and the phase B current fault flag is pushed high while the corresponding phase A fault flag remains low (Fig. 5,*b*).

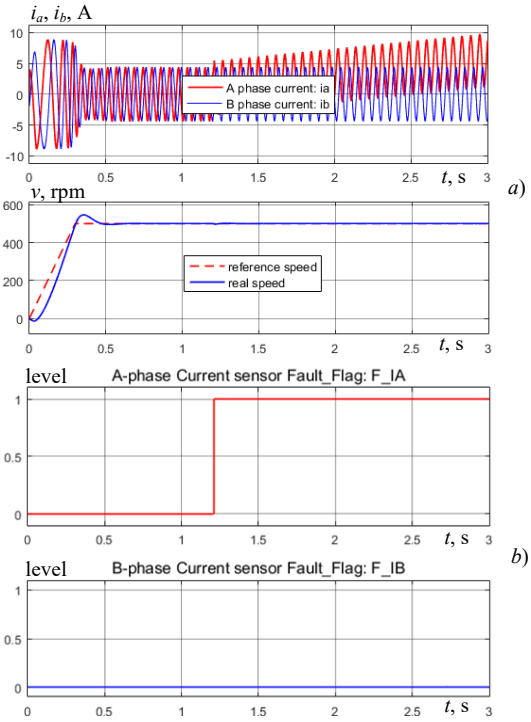

Fig. 4. FTC function according to the *drift* fault: (*a*) measured phase currents and motor speed; (*b*) the fault-indication-flags

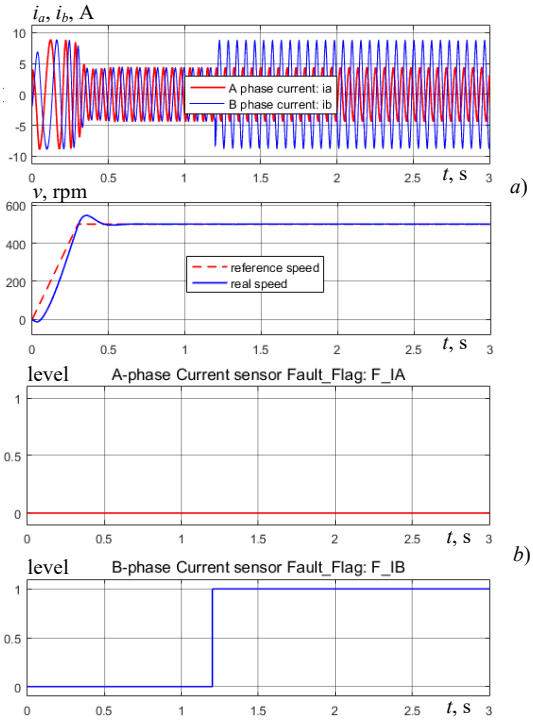

Fig. 5. FTC function according to the *scale* fault: (*a*) measured phase currents and motor speed; (*b*) the fault-indication-flags

In Fig. 6, the bias fault occurs at phase A (Fig. 6,*a*), the FTC function diagnoses the fault at phase A, and the phase B fault flag remains low (Fig. 6,*b*).

In Fig. 7, the final fault in the soft fault group, the precision degradation fault, occurs at phase B (Fig. 7,*a*), and the FTC function operates precisely according to the proper indication fault flags (Fig. 7,*b*).

Next simulation cases corresponding hard fault types: a constant feedback value of the phase A current corresponds to a value of 3 A (Fig. 8,*a*), constant feedback value with noise, phase B current value is a noise around the value 3 A (Fig. 9,*a*), bottom noise is around zero in phase A (Fig. 10,*a*). The FTC function accurately identified the faulty sensor locations in Fig. 8,*b*, 9,*b*, and 10,*b*, respectively. The estimated current is used instead of the measured current to supply the FOC loop and control the motor speed stably and accurately.

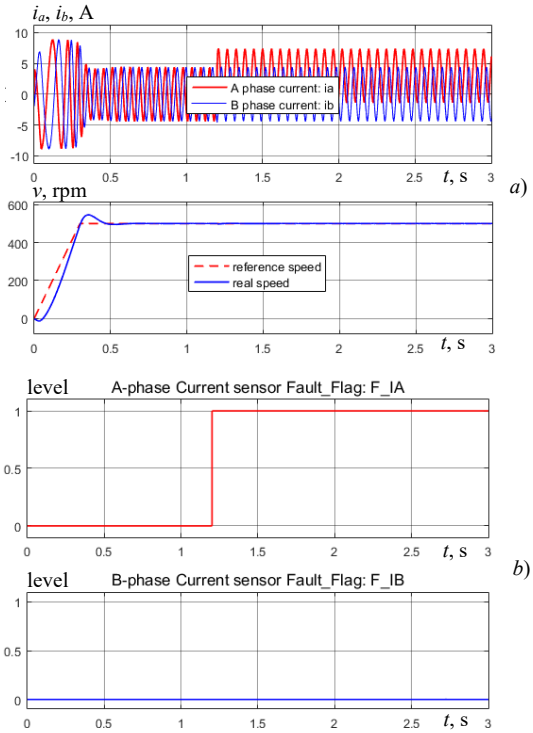

Fig. 6. FTC function according to the *bias* fault: (*a*) measured phase currents and motor speed; (*b*) the fault-indication-flags

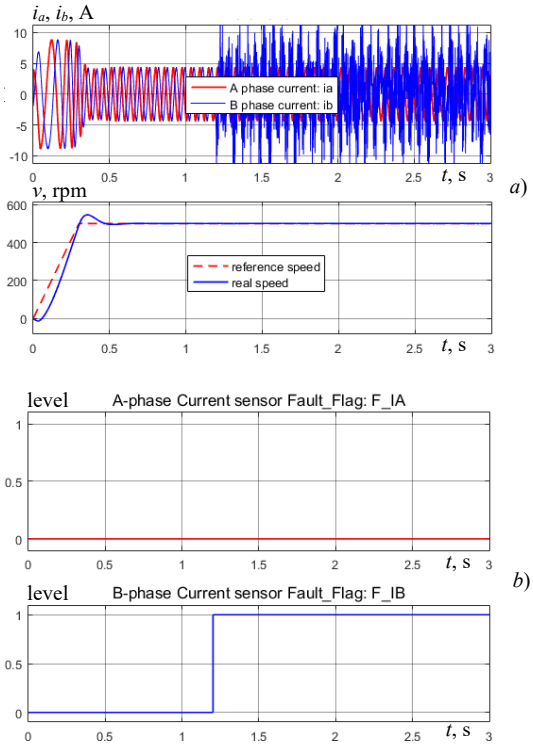

Fig. 7. FTC function according to the *precision degradation fault*: (*a*) measured phase currents and motor speed; (*b*) the fault-indication-flags

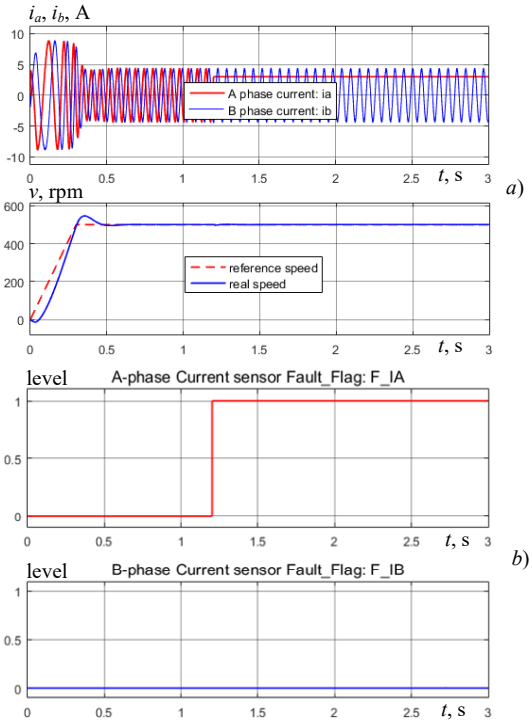

Fig. 8. FTC function according to the *constant feedback value*: (*a*) measured phase currents and motor speed; (*b*) the fault-indication-flags

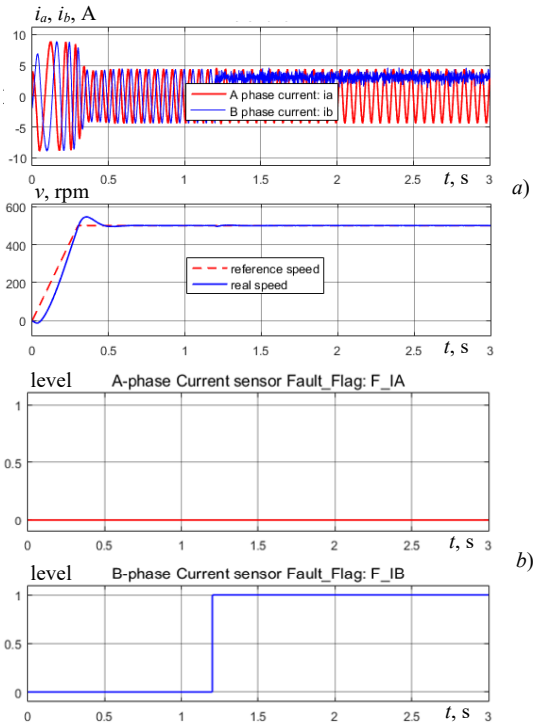

Fig. 9. FTC function according to the *constant feedback value with noise*: (*a*) measured phase currents and motor speed; (*b*) the fault-indication-flags

Conclusions. A hybrid method combining a third difference operator for the measured rotor speed and comparison algorithms of phase current signals is proposed to be applied to induction motor drive against various current sensor fault types. The third difference operator is used to check the signal quality status of the measured speed to ensure the estimated current calculated from the measured speed is accurate.

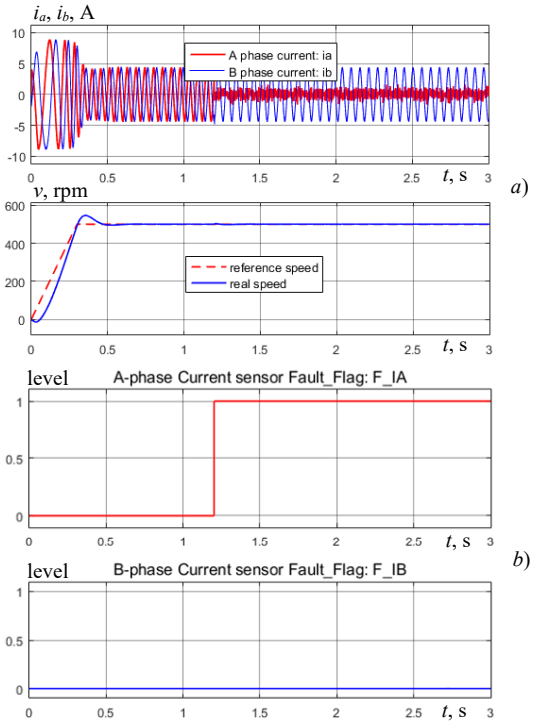

Fig. 10. FTC function according to the *bottom noise*: (*a*) measured phase currents and motor speed; (*b*) the fault-indication-flags

Then, the comparison algorithm between the measured and the estimated signals of each current phase is used to determine whether a discrepancy occurs or not. After determining the healthy status of each current sensor, if both current sensors are healthy, the measured currents are sent to the field-oriented control loop. If a failure occurs with any current sensors, the feedback signal corresponds to the estimated currents.

Through the results achieved, the proposed fault-tolerant control method has proven to be effective in accurately determining the health and location of the faulty phase currents in all simulation cases. The induction motor drive has enhanced stability and reliability in the motor control process, corresponding to the current sensor's health status.

Acknowledgment. Authors thank Ton Duc Thang University and VSB-Technical University of Ostrava for supporting. This research was funded by the European Union under the REFRESH – Research Excellence For REgion Sustainability and High-tech Industries project number CZ.10.03.01/00/22_003/0000048 via the Operational Programme Just Transition and by the Student Grant Competition of VSB-Technical University of Ostrava, grant number SP2024/051.

Conflict of interest. The authors declare that they have no conflicts of interest.

REFERENCES

1. Chan T., Shi K. *Applied Intelligent Control of Induction Motor Drives*. John Wiley & Sons (Asia) Pte Ltd, 2011. 421 p. doi: https://doi.org/10.1002/9780470825587.

2. Ibrar A., Ahmad S., Safdar A., Haroon N. Efficiency enhancement strategy implementation in hybrid electric vehicles using sliding mode control. *Electrical Engineering & Electromechanics*, 2023, no. 1, pp. 10-19. doi: https://doi.org/10.20998/2074-272X.2023.1.02.

3. Pena J.M., Diaz E.V. Implementation of V/f scalar control for speed regulation of a three-phase induction motor. *2016 IEEE ANDESCON*, 2016, pp. 1-4. doi: https://doi.org/10.1109/ANDESCON.2016.7836196.

4. Zhang Z., Bazzi A.M. Robust Sensorless Scalar Control of Induction Motor Drives with Torque Capability Enhancement at Low Speeds. *2019 IEEE International Electric Machines & Drives Conference (IEMDC)*, 2019, pp. 1706-1710. doi: https://doi.org/10.1109/IEMDC.2019.8785159.
5. Mon-Nzongo D.L., Jin T., Ekemb G., Bitjoka L. Decoupling Network of Field-Oriented Control in Variable-Frequency Drives. *IEEE Transactions on Industrial Electronics*, 2017, vol. 64, no. 7, pp. 5746-5750. doi: https://doi.org/10.1109/TIE.2017.2674614.
6. Zerdali E. A Comparative Study on Adaptive EKF Observers for State and Parameter Estimation of Induction Motor. *IEEE Transactions on Energy Conversion*, 2020, vol. 35, no. 3, pp. 1443-1452. doi: https://doi.org/10.1109/TEC.2020.2979850.
7. Tran C.D., Kuchar M., Sobek M., Sotola V., Dinh B.H. Sensor Fault Diagnosis Method Based on Rotor Slip Applied to Induction Motor Drive. *Sensors*, 2022, vol. 22, no. 22, art. no. 8636. doi: https://doi.org/10.3390/s22228636.
8. Amin A.A., Hasan K.M. A review of Fault Tolerant Control Systems: Advancements and applications. *Measurement*, 2019, vol. 143, pp. 58-68. doi: https://doi.org/10.1016/j.measurement.2019.04.083.
9. Moussaoui L., Aouaouda S., Rouaibia R. Fault tolerant control of a permanent magnet synchronous machine using multiple constraints Takagi-Sugeno approach. *Electrical Engineering & Electromechanics*, 2022, no. 6, pp. 22-27. doi: https://doi.org/10.20998/2074-272X.2022.6.04.
10. Gouichiche A., Safa A., Chibani A., Tadjine M. Global fault-tolerant control approach for vector control of an induction motor. *International Transactions on Electrical Energy Systems*, 2020, vol. 30, no. 8, art. no. e12440. doi: https://doi.org/10.1002/2050-7038.12440.
11. Wang Z., Shao J., He Z. Fault Tolerant Sensorless Control Strategy With Multi-States Switching Method for In-Wheel Electric Vehicle. *IEEE Access*, 2021, no. 9, pp. 61150-61158. doi: https://doi.org/10.1109/ACCESS.2021.3072700.
12. Chaabane H., Khodja D.E., Chakroune S., Hadji D. Model reference adaptive backstepping control of double star induction machine with extended Kalman sensorless control. *Electrical Engineering & Electromechanics*, 2022, no. 4, pp. 3-11. doi: https://doi.org/10.20998/2074-272X.2022.4.01.
13. Gundewar S.K., Kane P.V. Condition Monitoring and Fault Diagnosis of Induction Motor. *Journal of Vibration Engineering & Technologies*, 2021, vol. 9, no. 4, pp. 643-674. doi: https://doi.org/10.1007/s42417-020-00253-y.
14. Niu G., Xiong L., Qin X., Pecht M. Fault detection isolation and diagnosis of multi-axle speed sensors for high-speed trains. *Mechanical Systems and Signal Processing*, 2019, vol. 131, pp. 183-198. doi: https://doi.org/10.1016/j.ymssp.2019.05.053.
15. Azzoug Y., Menacer A., Pusca R., Romary R., Ameid T., Ammar A. Fault Tolerant Control for Speed Sensor Failure in Induction Motor Drive based on Direct Torque Control and Adaptive Stator Flux Observer. *2018 International Conference on Applied and Theoretical Electricity (ICATE)*, 2018, pp. 1-6. doi: https://doi.org/10.1109/ICATE.2018.8551478.
16. Manohar M., Das S. Notice of Removal: Current Sensor Fault-Tolerant Control of Induction Motor Driven Electric Vehicle Using Flux-Linkage Observer. *2020 IEEE Transportation Electrification Conference & Expo (ITEC)*, 2020, pp. 884-889. doi: https://doi.org/10.1109/ITEC48692.2020.9161553.
17. Aib A., Khodja D.E., Chakroune S., Rahali H. Fuzzy current analysis-based fault diagnostic of induction motor using hardware co-simulation with field programmable gate array. *Electrical Engineering & Electromechanics*, 2023, no. 6, pp. 3-9. doi: https://doi.org/10.20998/2074-272X.2023.6.01.
18. Gholipour A., Ghanbari M., Alibeiki E., Jannati M. Speed sensorless fault-tolerant control of induction motor drives against current sensor fault. *Electrical Engineering*, 2021, vol. 103, no. 3, pp. 1493-1513. doi: https://doi.org/10.1007/s00202-020-01179-0.
19. Manohar M., Das S. Current Sensor Fault-Tolerant Control for Direct Torque Control of Induction Motor Drive Using Flux-Linkage Observer. *IEEE Transactions on Industrial Informatics*, 2017, vol. 13, no. 6, pp. 2824-2833. doi: https://doi.org/10.1109/TII.2017.2714675.
20. Zuo Y., Ge X., Chang Y., Chen Y., Xie D., Wang H., Woldegiorgis A.T. Current Sensor Fault-Tolerant Control for Speed-Sensorless Induction Motor Drives Based on the SEPLL Current Reconstruction Scheme. *IEEE Transactions on Industry Applications*, 2023, vol. 59, no. 1, pp. 845-856. doi: https://doi.org/10.1109/TIA.2022.3204733.
21. Huu Nguyen M.C., Tran C.D. An extended sensor fault tolerant control method applied to three-phase induction motor drives. *Bulletin of Electrical Engineering and Informatics*, 2024, vol. 13, no. 1, pp. 125-133. doi: https://doi.org/10.11591/eei.v13i1.5992.
22. Yi T.-H., Huang H.-B., Li H.-N. Development of sensor validation methodologies for structural health monitoring: A comprehensive review. *Measurement*, 2017, vol. 109, pp. 200-214. doi: https://doi.org/10.1016/j.measurement.2017.05.064.
23. Tran C.D., Nguyen T.X., Nguyen P.D. A field-oriented control (FOC) method using the virtual currents for the induction motor drive. *International Journal of Power Electronics and Drive Systems (IJPEDS)*, 2021, vol. 12, no. 4, pp. 2095-2102. doi: https://doi.org/10.11591/ijpeds.v12.i4.pp2095-2102.
24. Ho S.D., Brandstetter P., Palacky P., Kuchar M., Dinh B.H., Tran C.D. Current sensorless method based on field-oriented control in induction motor drive. *Journal of Electrical Systems*, 2021, vol. 17, no. 1, pp. 62-76.
25. Adamczyk M., Orlowska-Kowalska T. Self-Correcting Virtual Current Sensor Based on the Modified Luenberger Observer for Fault-Tolerant Induction Motor Drive. *Energies*, 2021, vol. 14, no. 20, art. no. 6767. doi: https://doi.org/10.3390/en14206767.
26. Azzoug Y., Pusca R., Sahraoui M., Ammar A., Romary R., Marques Cardoso A.J. A Single Observer for Currents Estimation in Sensor's Fault-Tolerant Control of Induction Motor Drives. *2019 International Conference on Applied Automation and Industrial Diagnostics (ICAAID)*, 2019, pp. 1-6. doi: https://doi.org/10.1109/ICAAID.2019.8934969.
27. Rahman T., Motakabber S.M.A., Ibrahimy M.I. Design of a Switching Mode Three Phase Inverter. *2016 International Conference on Computer and Communication Engineering (ICCCE)*, 2016, pp. 155-160. doi: https://doi.org/10.1109/ICCCE.2016.43.
28. Adamczyk M., Orlowska-Kowalska T. Postfault Direct Field-Oriented Control of Induction Motor Drive Using Adaptive Virtual Current Sensor. *IEEE Transactions on Industrial Electronics*, 2022, vol. 69, no. 4, pp. 3418-3427. doi: https://doi.org/10.1109/TIE.2021.3075863.
29. Azzoug Y., Sahraoui M., Pusca R., Ameid T., Romary R., Cardoso A.J.M. High-performance vector control without AC phase current sensors for induction motor drives: Simulation and real-time implementation. *ISA Transactions*, 2021, vol. 109, pp. 295-306. doi: https://doi.org/10.1016/j.isatra.2020.09.021.

Received 05.05.2024
Accepted 18.08.2024
Published 21.10.2024

C.D. Tran[1]*, Doctor on Electrical Engineering,*
M. Kuchar[2]*, Professor, Doctor on Electrical Engineering,*
P.D. Nguyen[2,3]*, PhD Student,*
[1] Power System Optimization Research Group,
Faculty of Electrical and Electronics Engineering,
Ton Duc Thang University, Ho Chi Minh City, Vietnam,
e-mail: trandinhcuong@tdtu.edu.vn (Corresponding Author)
[2] Department of Applied Electronics,
Faculty of Electrical Engineering and Computer Science,
VSB-Technical University of Ostrava, Czech Republic,
e-mail: martin.kuchar@vsb.cz; phuong.nguyen.duy.st@vsb.cz
[3] Faculty of Electronics and Telecommunication,
Saigon University, Ho Chi Minh City, Vietnam,
e-mail: phuong.nd@sgu.edu.vn

How to cite this article:
Tran C.D., Kuchar M., Nguyen P.D. Research for an enhanced fault-tolerant solution against the current sensor fault types in induction motor drives. *Electrical Engineering & Electromechanics*, 2024, no. 6, pp. 27-32. doi: https://doi.org/10.20998/2074-272X.2024.6.04